Mobile Human Airbag System for Fall Protection Using MEMS Sensors and Embedded SVM Classifier

Guangyi Shi, Cheung Shing Chan, Wen Jung Li, Kwok-Sui Leung, Yuexian Zou, and Yufeng Jin

***Abstract*—This paper introduces a mobile human airbag system designed for fall protection for the elderly. A Micro Inertial Measurement Unit (μIMU) of 56 mm $\times$ 23 mm $\times$ 15 mm in size is built. This unit consists of three dimensional MEMS accelerometers, gyroscopes, a Bluetooth module and a Micro Controller Unit (MCU). It records human motion information, and, through the analysis of falls using a high-speed camera, a lateral fall can be determined by gyro threshold. A human motion database that includes falls and other normal motions (walking, running, etc.) is set up. Using a support vector machine (SVM) training process, we can classify falls and other normal motions successfully with a SVM filter. Based on the SVM filter, an embedded digital signal processing (DSP) system is developed for real-time fall detection. In addition, a smart mechanical airbag deployment system is finalized. The response time for the mechanical trigger is 0.133 s, which allows enough time for compressed air to be released before a person falls to the ground. The integrated system is tested and the feasibility of the airbag system for real-time fall protection is demonstrated.**

***Index Terms*—Digital signal processing (DSP), human motion sensing, microelectromechanical systems (MEMS), μ inertial measurement unit (μIMU), mobile airbags, support vector machine (SVM).**

I. Introduction

THE WORLD is faced with an increasingly aging population. Along with this increase, the proportion of elderly people who are frail and dependent is also likely to rise significantly [1]. Given that falls and fall-induced fractures are very common among the elderly, this shift in demographic patterns will lead to an exponential increase in the number of elderly individuals who suffer injuries from falls.

Hip fractures account for most of the deaths and costs associated with fall-induced fractures. Worldwide, there are around 4 000 000 hip fracture cases every year, and the annual mortality rate is 30.8%. In Hong Kong, there are 4000 hip fracture cases per year [2]. The annual medical and rehabilitation expenditure associated with these cases amounts to HK$150 million. Many hip protectors composed of a pair of hard pads worn with a tight undergarment are commercially available. Some of these protectors have been proven to have a force attenuation ability of as high as 95% [3]. However, because the elderly find such protectors uncomfortable and inconvenient, they have a poor compliance rate and do not deliver the hip fracture prevention qualities expected of them. In Hong Kong, hot weather is a significant factor in the low compliance rate, which averages 40% for the entire year and ranges from 70% in the autumn to 20% in the summer [4].

To build a protective system, the concept underlying automobile airbag systems is applied. This system has two modules: a sensing module (μIMU) and an inflator connected to two nylon airbags. When the μIMU detects a fall, it triggers an inflator, which then deploys the airbags before impact to protect the wearer. The gas is supplied from a handy compressed gas cylinder, rather than relying on the combustion of chemicals.

Due to the availability of small, low-cost microelectromechanical systems (MEMS) sensors, it is possible to build self-contained inertial sensors with an overall system dimension of less than 1 cubic inch and, at the same time, a sensing unit that can track disorientation and other motions in real time. The real-time monitoring of human movement can be employed to facilitate long-term monitoring [5]. Previous studies have also demonstrated the use of similar units to recognize daily life activities and acquire indirect measures of metabolic energy expenditure [6]. Some papers have presented the implementation of a real-time classification system for the types of human movement that are associated with motion sensing data [7]. The sampling rate for this system is too low, and it is only suitable for normal life recording and analysis. Few μIMU systems are designed for real-time interaction with humans and mechanistic systems for other types of action.

Our group has developed a Micro Input Device System (MIDS) based on MEMS sensors as a novel multifunctional interface input system that could potentially replace the mouse, pen, and keyboard as input devices for computers [8], [9]. We have also developed a μIMU that measures three-dimensional angular rates and accelerations based on MEMS sensors. We have integrated a microcontroller and a Bluetooth module into the μIMU, and the overall size of the unit is less than 56 mm $\times$ 23 mm $\times$ 15 mm. We have developed the module as a ubiquitous wireless digital writing instrument that interacts with humans and computers [10]. A human airbag system is another application of this module. Along with the μIMU, the system includes a support vector machine (SVM) filter, an embedded DSP, and a mechanical system for airbag deployment.

This paper describes the implementation of the mobile human airbag system. First, the μIMU and the mechanical airbag deployment system were finalized. Based on an analysis using high-speed camera data, a gate filter was generated and fitted to the μIMU, and an independent airbag release experiment

Manuscript received May 08, 2008; revised July 27, 2008; accepted July 30, 2008. Current version published March 27, 2009. The associate editor coordinating the review of this paper and approving it for publication was Prof. Okyay Kaynak.

G. Shi, Y. Zou, and Y. Jun are with the Graduate School of Peking University, Shenzhen University Town, Xili, Shenzen, China.

C.-S. Chan and W. J. Li are with the Chinese University of Hong Kong, Hong Kong, China (e-mail: wen@mae.cuhk.edu.hk).

K.-S. Leung is with the Department of Orthopaedics and Traumatology, Chinese University of Hong Kong, Hong Kong, China, and also with the Prince of Wales Hospital, Shatin, Hong Kong, China.

Digital Object Identifier 10.1109/JSEN.2008.2012212

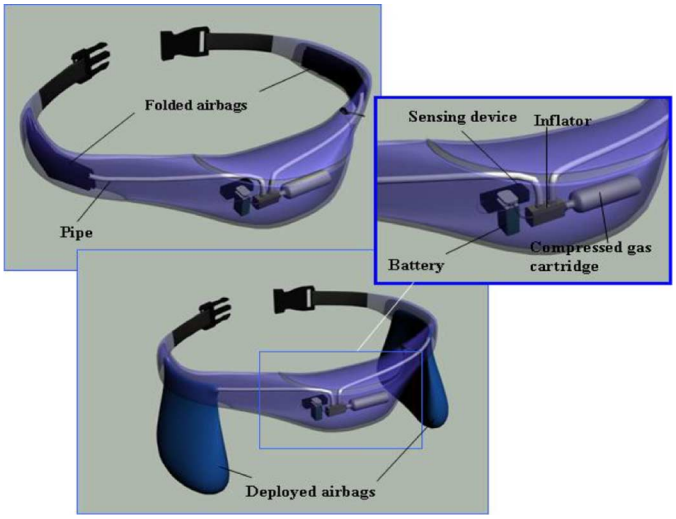

Fig. 1. Conceptual illustration of the "intelligent" human airbag system.

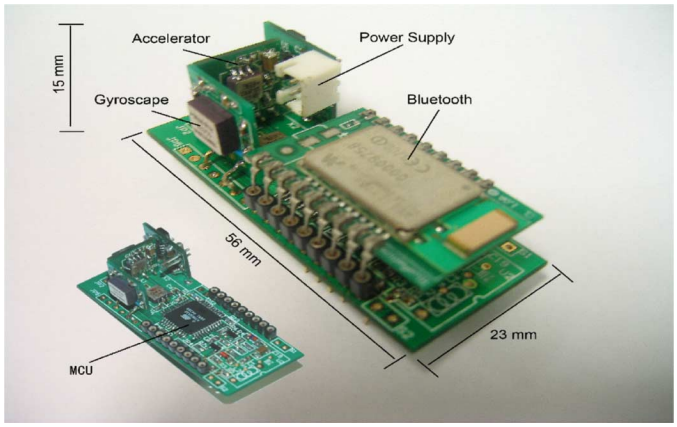

Fig. 2. Photograph of a 3-D motion sensing system consisting of three gyros and three accelerometer sensors.

showed that the μIMU combines well with the deployment system for hip protection. Second, SVM was introduced for the recognition of falls. We set up a database of 100 lateral falls and 100 other normal motions including walking, running, sitting, going upstairs and downstairs, taking an elevator and squatting. Using an SVM training process, an SVM filter capable of successfully classifying falls and other motions was generated. Third, a slide window process and a new SVM filter with a lower sampling rate were used for real-time fall recognition. After simulating the relevant algorithms, an embedded DSP system was used to show the classification of falls in real time, which proved the feasibility of our system.

This paper is organized as follows. In Section II, the airbag system as a whole is introduced, including μIMU hardware, the design of the deployment system and the independent demonstration based on high-speed camera analysis. Section III introduces the SVM process and Section IV presents real-time implementation of the SVM filter. Finally, our conclusions are presented in Section V.

II. A Human Airbag System for Fall Protection

As noted above, hip fractures account for most of the costs associated with falls and fall-induced fractures, especially among elderly people. We propose the development of intelligent and personalized wearable airbags to reduce the impact force of falls among the elderly. Fig. 1 illustrates the basic concept underlying the intelligent human airbag system. Initially, the airbag is compressed inside a belt. When an elderly person loses his or her balance, the MEMS microsensors in the belt detect his or her disorientation and trigger the inflation of the airbag on the appropriate side a few milliseconds before the person falls to the ground. There are two main parts to this project. The first is the electronic part that uses an algorithm to judge falls and sends a trigger signal to the airbag inflator. The second is the mechanical part, which includes the inflator structure for compression, airbag deployment control, and airbag design.

A. μIMU Design

MEMS sensors play a major role in the μIMU due to their low cost and miniature size. For our experiments, we use ADXL203 (AD Inc.) sensors as accelerometers [13] and muRata ENC-03 angular rate gyros, respectively. These are low-cost and relatively high-performance sensors with analog signal output. The output signals of the accelerometers (a_x, a_y, a_z) and the angular rate gyros $(\omega_x, \omega_y, \omega_z)$ are converted directly by an A/D converter inside the microcontroller. We use an ATMEL ATmega32 microcontroller in this design. This microcontroller has a 32 Kbyte flash, 2 Kbyte of SRAM, 8 channels of 10-bit ADC, and a USART (Universal Synchronous and Asynchronous serial Receiver and Transmitter) port [13]. The sampling rate of the microcontroller is 200 Hz, which ensures rapid reaction to human motion. We use a TDK Systems blu2i Module in our system to transfer data to a host system. This Bluetooth module allows for easy integration with various host systems. The module is directly connected to the microcontroller via a USART port. The module is very small (45 mm $\times$ 20 mm $\times$ 10 mm) and can easily communicate with the microcontroller.

The accelerometers and gyros act as a micro inertial measurement unit of the motion sensing system. These μIMU sensors and the Bluetooth module are housed in a small PCB, as shown in Fig. 2. According to the calculations, two 3.6 V Li batteries can power the unit for 8–10 h. The computer receives 3-D accelerations and angular rates, displays them in six time-domain plots, each of which represents an axis acceleration and rotation rate. At the same time, a text file consisting of six characters is generated for later analysis. The μIMU is thus capable of performing two functions: first, the capture and wireless transmission of data that can be analyzed later to the computer, and second, the downloading of an angular rate-based recognition algorithm used to identify a falling motion and trigger the airbag for inflation.

B. Airbag Release System

The mechanical release mechanism (Fig. 3) includes a cross-shaped punch mounted on a launcher that consists of a spring and a locking switch. The spring is compressed by screwing. When the locking switch is pressed by an actuator, the compressed spring extends and the punch accelerates toward the pressurized cylinder. The compressed CO_2 is released from the gap between the punch and the cylinder cap. Finally, the gas is transmitted along a 16-cm-long pipe to inflate the airbag.

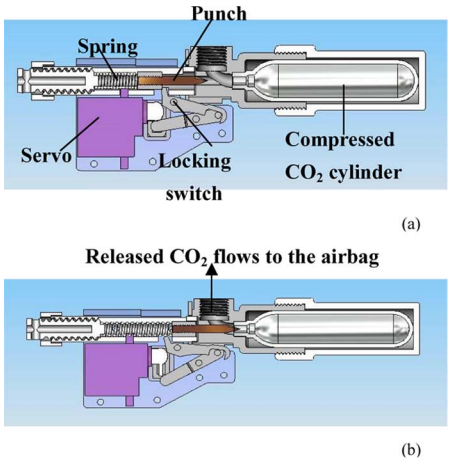

Fig. 3. The cross-sectional view of the inflator: (a) state before triggering; (b) after triggering, gas is released.

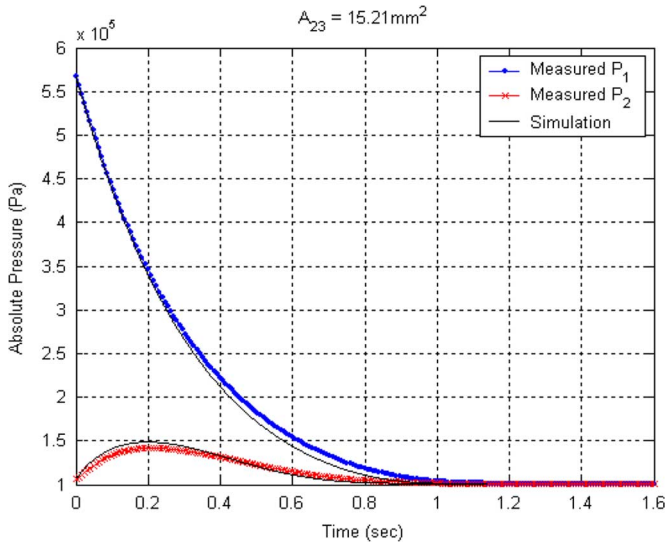

Fig. 4. Comparison of experimental and simulation results for mobile airbag inflation (pressure versus time).

The actuator used is a 16 g commercially available servo BMS-380MAX of $26 \times 13 \times 26$ mm in size, with a speed of 0.15 s/60° at 4.8 V. It requires only 5 V and less than 0.6 A. The maximum torque is 4.1 kg/cm at 4.8 V. It can easily be driven by the microcontroller with pulse-width modulation (PWM), which controls the position of the servo angle according to the length of the pulse form. Its response time (from the time the servo receives a signal until the compressed gas is first released) consistently lies between 0.1 and 0.133 s.

We have also engineered the airbag inflation process to ensure that the airbags can be inflated within 0.333 s. This means that the entire process of fall detection, mechanical triggering and airbag inflation must be completed within 0.9 s in order for the system to protect the wearer. Classical compressible-fluid mass flow rate equations are used to estimate flow parameters through an orifice

$$W_{12} = \frac{A_{12}P_1}{\sqrt{T_1}} \left\{ \frac{2\gamma}{R(\gamma-1)} \left[\left(\frac{P_2}{P_1}\right)^{2/\gamma} - \left(\frac{P_2}{P_1}\right)^{\gamma+1/\gamma} \right] \right\}^{1/2} \left(\frac{P_2}{P_1} > 0.528\right)$$

$$W_{12} = \frac{A_{12}P_1}{\sqrt{T_1}} \left\{ \frac{\gamma}{R} \left[\left(\frac{2}{\gamma+1}\right)^{(\gamma+1)/(\gamma-1)} \right] \right\}^{1/2} \times \left(\frac{P_2}{P_1} \le 0.528\right) \quad (1)$$

where W is mass flow rate (kg/s), A_{12} is the area of the airbag inlet orifice (in m^2), P_1 and P_2 are cylinder pressure and airbag pressure respectively, which are used to determine final air pressure (as recorded by a pressure sensor), γ is the specific heat ratio ($\gamma = 1.4$ for air, 1.3 for CO_2) and R is the gas constant ($R = 287$ j/kgK for air, 188.9 j/kgK for CO_2). The equations shown below describe instantaneous pressure in the compressed gas cylinder under subsonic flow and sonic flow, respectively

$$\frac{dP_1}{P_1} = -N_{12}d\left(\frac{KR\sqrt{T_0}A_{12}}{V_1}t\right) = -N_{12}d\tau$$
$$P_1 = P_0 e^{-\tau} \quad (2)$$

where $\tau = (KR\sqrt{T_0}A_{12})/(V_1)t$ and N_{12} is the ratio of mass flow rate to choked mass flow rate. For subsonic flow, N_{12} varies with the pressure ratio and the differential equation is solved using Matlab Simulink. Fig. 4 shows a comparison between the pressures derived through simulation and those calculated from experimental results (using an outlet orifice of 15.21 mm^2 at an initial pressure of 550 kPa). It is clear that the above equations are suitable for modeling gas flow parameters during the airbag inflation process.

For the implementation of the human airbag system, we found that a 12g CO_2 cartridge (with a diameter of 8 mm and a total length of 85 mm) could be used to expand a 1.88×10^{-3} m^3 airbag (the minimum dimensions of an airbag for effective impact reduction). According to the calculations, the ratio of CO_2 mass supplied (M_s) and the gas mass required for the desired airbag volume (M_a) is $1.057 > 1$, which means the CO_2 from a 12 g cartridge can be used to inflate an airbag to the minimum volume required to protect the wearer within 0.333 s. The compact nature of the CO_2 cartridge and airbag makes the system suitable for everyday use among the elderly.

C. High-Speed Camera Analyses and Airbag System Demo

To analyze the μIMU signal output, a high-speed camera was used to record the falling motion, while the μIMU was in operation. The camera model used was a PCO 1200 hs High-Speed Cam with a maximum resolution of 1280×1025 pixels. The film rate used was 200 Hz. The camera was placed 5 m from the subject in a position orthogonal to the direction of the fall. By measuring the inclined angle of the trunk (θ_i) in the frames within the known time interval, the change in the inclined angle with respect to time can be obtained. The angle-time relationship can be fitted with a cubic curve. The instantaneous angular velocity of the hip can be measured by differentiating this cubic curve. Moreover, when compared to one of the gyro outputs (the rotational velocity of the trunk) of the μIMU, the signal corresponding to impact can be justified. In Fig. 5, the inclined angle of the trunk (θ_i) is measured from the film produced by

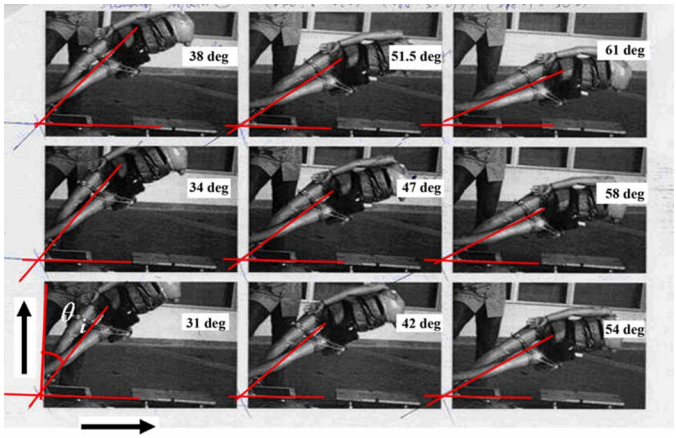

Fig. 5. Fall analysis with high-speed camera.

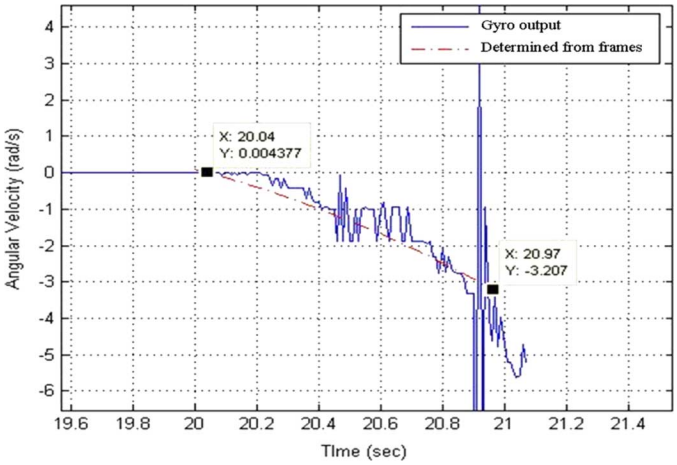

Fig. 6. Comparison of high-speed camera results and the gyro sensor output.

the high-speed camera. θ_i is determined from the feature represented by the horizontal line in the film.

As shown in Fig. 6, when we compared the high-speed camera results with one of the gyro outputs (the rotational velocity of the trunk) of the μIMU, the signal corresponding to impact could be justified. The gyro output was very similar to the image analysis. This also helped us to determine when we should open the airbag.

Using the results from the high-speed camera and the inflator, we were able to set up a demo to show the feasibility of the airbag system. We connected the air cartridge to the inflator and the inflator to the μIMU. The inflator is used to trigger the μIMU. A certain gyro sensor value was set as the threshold for a dangerous fall. Given that we assumed that after a 30° angle, a person cannot maintain his or her balance any longer, we traced the value of angular velocity from the high-speed camera results and input it into the gyro sensor. When the gyro sensor output following an action is bigger than this value, the μIMU triggers the airbag.

Fig. 7 shows the results of airbag deployment. When a person is falling and the angular velocity is larger than a given value, the sensor module triggers the CO_2 cylinder to release air and inflate the airbag. It can clearly be seen that the airbag is inflated before

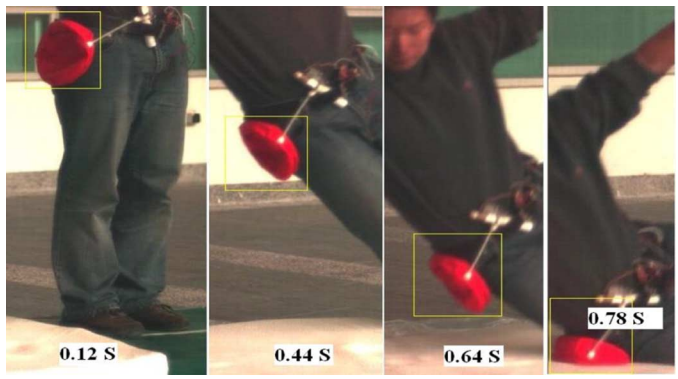

Fig. 7. Independent demonstration with μIMU and deployment system.

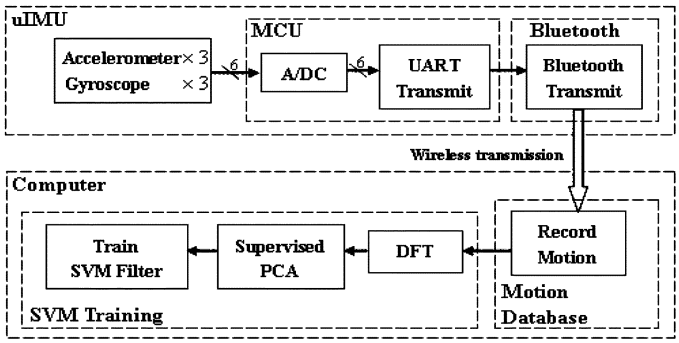

Fig. 8. Schematic chart of SVM training.

the person falls to the ground, which provides hip protection. This experiment proves that the airbag system is feasible.

III. SVM Classification

Although a simple angular rate threshold can be used to indicate that a fall is in progress, false inflations can occur during normal physical activity. This emphasizes the need to make the trigger device reliable, such that the sensing unit triggers the deployment system when a fall occurs, and at the same time, false signals that induce unnecessary panic are not generated, a feature especially important to the elderly. The SVM, a kind of neural network algorithm, was selected because it is a good binary classifier that requires a relatively low number of samples. A SVM-based scheme using a host computer was tested to distinguish between normal and falling motions.

As shown in Fig. 8, the MCU first converts the sensor outputs into digital signals and then transmits the packed data signal sequentially via a Bluetooth module to a computer. Hundreds of recordings, including lateral falls, walking, running, sitting, walking up and down stairs, and stepping into elevators, were made to form a database for SVM training. After training, we selected the best features to form a classifier for falling-motion recognition.

Our goal is to facilitate the recognition of a falling-down motion in real time and control a hip-protection airbag. We addressed this problem through the use of binary pattern recognition with SVM, as follows.

1) Setting up a database of "falling down" and "non-falling-down" motions through experiments in which the uIMU was worn.

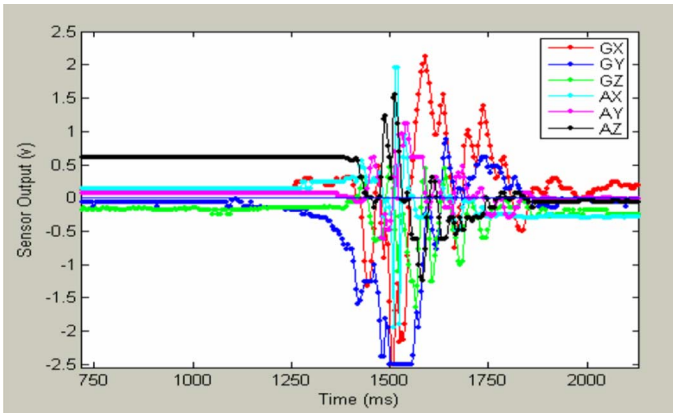

Fig. 9. Original data recorded for a falling down motion.

2) Using supervised principal component analysis (PCA) to generate and select characteristic features.
3) Using SVM training to derive the SVM classifier.

A. Database Setup

Two groups of experiments were carried out. These involved one hundred lateral falls and one hundred other motions, including 10 running motions, 20 walking motions, 20 sitting motions, 20 squatting motions, 20 motions involving walking up or down stairs, and 10 jumping motions. These motions were selected as normal motions undertaken in everyday life. Because the elderly seldom jump or run, we collected more data on sitting and squatting motions, an approach that can also be justified on the basis that these motions are more similar to the motions that occur during a fall.

Fig. 9 shows the original data for one falling motion, including the 3-D accelerations and rotation rates from one experimental trial. In Fig. 9, GY (represented by the blue line) is the angular rate of the pitch direction, the change in which gives a starting point for judging a falling motion. AZ (the black line) represents vertical acceleration. The sudden spike in the data corresponds to the point in time at which the hip hits the ground. By synchronizing visual observations with the sensed data, we extracted motion data from the beginning of a fall to when the body hit the ground (a soft mat) for all six sensors.

One hundred experimental falls were carried out, including fast and slow falling motions. The experiments involved the used of two different people as models to allow for the construction of a more realistic database. The same cuttings were also done for the 100 normal motions. This resulted in the formation of a database of 100 falls and 100 normal motions.

B. Supervised PCA and ICA for Feature Extraction

Feature generation and selection are very important in falling down recognition, as badly selected features such as weightlessness, leaning backward and hip spinning may be confused with jumping, sitting and turning around, which can clearly reduce the effectiveness of the system. Furthermore, although the present features contain enough information about the output class, they may not predict the output correctly, because the spatial dimensions of a feature may be so large that numerous instances are required to determine the result.

PCA can be used to generate mutually uncorrelated features while packing most of the relevant information into several eigenvectors. In our system, we use supervised PCA algorithms to generate features and select high-quality combinations for better recognition performance.

A set of eigenvectors can be computed from the training motion data and some of eigenvectors were selected for classification according to the corresponding eigenvalue.

We selected the eigenvectors according to binary classified capability rather than according to the corresponding eigenvalues. This is because while the eigenvectors with large eigenvalues may carry the common features, they do not carry the information required for distinguishing between two classes.

The method can be described as follows. Suppose that we have two sets of training samples: A and B. The number of training samples in each set is N. Φ_i represents each eigenvector produced through PCA. Each of the training samples, including both positive samples and negative samples, can be projected into an axis extended by the corresponding eigenvector. By analyzing the distribution of the projected $2N$ points, we can roughly select those eigenvectors which have more motion information. The following is a detailed description of the process.

1) For a certain eigenvector Φ_i, compute its mapping result according to the two sets of training samples. The result can be described as $\lambda_{i,j}, (1 \le i \le M, 1 \le j \le 2N)$. M is the number of eigenvectors and $2N$ is the total number of training samples.
2) Train a classifier f_i using a simple method, such as Perception or Neural Network, which can be used to separate $\lambda_{i,j}$ into two groups, falling down and non-falling-down, with a minimum error $E(f_i)$.
3) If $E(fi) < \varepsilon$, select this eigenvector from the original set of eigenvectors. ε is the defined threshold. The selected eigenvectors can also be represented back to motion data representing a typical movement.

Independent component analysis (ICA) is then used to take a set of observations and find a group of independent components that explain the data. PCA considers the second-order moments only and uncorrelates data, while ICA accounts for higher order statistics and thus provides a more powerful data expression than PCA [11].

Here, we randomly select three of the selected eigenvectors generated through the supervised PCA process to form parameter matrix P. When P is multiplied by A and B, two input matrices are generated which contain only three parameters for each input vector, which we call $\bar{A}$ and $\bar{B}$. When we follow the ICA process in [11], good P is selected and the corresponding $\bar{A}$ and $\bar{B}$ are selected as the training inputs for the SVM process.

C. SVM Training Process

Our goal is to separate the original data into two classes, falls and normal motions, according to a group of features. In our system, the input data for human motion is high dimensional and nonlinear. We have to map the data represented by $\bar{A}$ and $\bar{B}$ into a high-dimensional feature space F via a nonlinear mapping Φ, and do linear regression in this space [12]. We assume that the

input vectors are $\bar{\mathbf{x}}_1, \bar{\mathbf{x}}_2, \ldots, \bar{\mathbf{x}}_N$ and that $\mathbf{z}_i \in \{1, -1\}$ is the class label of $\bar{\mathbf{x}}_i$

$$f(\bar{\mathrm{x}}) = (\omega \cdot \Phi(\bar{\mathbf{x}})) + \mathrm{b} \quad (\Phi : R^3 \to F, \omega \in F). \tag{3}$$

Thus, linear regression in a high-dimensional (feature) space corresponds to nonlinear regression in the low-dimensional input space R^3. Note that b is the threshold and the dot product between ω and $\Phi(\bar{\mathbf{x}})$ has to be computed in this high-dimensional space (which is usually intractable) if we are not able to use the kernel that eventually leaves us with dot products that can be implicitly expressed in the low-dimensional input space R^3. The kernel function is defined by

$$K(\bar{\mathbf{x}}_\mathrm{i}, \bar{\mathbf{x}}_\mathrm{j}) = \Phi(\bar{\mathbf{x}}_i)^T \Phi(\bar{\mathbf{x}}_j). \tag{4}$$

As explained in [12], any symmetric kernel function K that satisfies Mercer's condition corresponds to a dot product in some feature space. As a detailed reference on the theory and computation of SVM, readers can refer to [12]. There are many kernels that satisfy Mercer's condition as described in [12]. In this paper, we take a simple polynomial kernel

$$K(\bar{\mathbf{x}}_i, \bar{\mathbf{x}}) = ((\bar{\mathbf{x}}_i \cdot \bar{\mathbf{x}}) + 1)^d. \tag{5}$$

Thus, we should solve

$$\begin{aligned} &\max . \varpi(\alpha) = \sum_{i=1}^{n} \alpha_i \\ &\quad - \frac{1}{2} \sum_{i=1, j=1}^{n} \alpha_i \alpha_j \mathbf{z}_i \mathbf{z}_j K(\bar{\mathbf{x}}_i, \bar{\mathbf{x}}_j) \\ &\text{subject to } \xi \geq \alpha_i \geq 0, \sum_{i=1}^{n} \alpha_i \mathbf{z}_i = 0 \end{aligned} \tag{6}$$

where ξ is a tradeoff parameter between error and margin and α_i are Lagrangian multipliers. This is a quadratic programming (QP) problem with a selected kernel function in which the α_i can be calculated and the relative input vectors are called the support vectors. Given that a lot of Lagrangian multipliers will go to zero, there are only a few (denoted as l) support vectors left for the calculation of b through the following equations:

$$\omega = \sum_{j=1}^{l} \alpha_j \mathbf{z}_j \Phi(\bar{\mathbf{x}})_j \tag{7}$$

$$\begin{aligned} f &= \langle \omega, \phi(\bar{\mathbf{x}}) \rangle + b \\ &= \sum_{j=1}^{l} \alpha_j \mathbf{z}_j K(\bar{\mathbf{x}}_j, \bar{\mathbf{x}}) + b. \end{aligned} \tag{8}$$

D. SVM Training and Experimental Results

Two hundred experimental results consisting of an even split of "falling down" data and "non-falling-down" data were recorded. Each result consisted of six arrays measured by the six respective sensors.

Data preprocessing was performed to filter noise and reduce dimension. For each experimental result, we performed a DFT of the six respective arrays and kept the first ten coefficients of each DFT result. After 200 DFTs, we obtained a matrix of 200 rows and 60 columns, each row representing an experiment. Each had $6 * 10$ numbers in the sequence Gx, Gy, Gz, Ax, Ay, Az.

TABLE I
THE COEFFICIENTS OF THE SVM CLASSIFIER

c_0	-4.114032908	c_5	-0.000013017
c_1	0.029363568	c_6	0.000056986
c_2	0.009281220	c_7	0.000004560
c_3	0.004760046	c_8	-0.000013625
c_4	-0.000004642	c_9	0.000052657

It was found that compressing the training data into three dimensions using PCA and ICA was sufficient to obtain good classification results. We randomly chose half of the data for SVM training and the other half was used for testing.

For the unseen testing data, good results were obtained. Basically, the resulting system could classify the test vectors into 'falling-down" and "non-falling-down" states with 100% accuracy.

The computation required for the SVM classifier is shown in (7). The corresponding coefficients are shown in Table I. Although the training process is computationally expensive, after training, the computational requirements of the classifier are very small

$$\begin{aligned} f(x_1, x_2, x_3) = {} & c_0 + c_1 \cdot x_1 + c_2 \cdot x_2 \\ & + c_3 \cdot x_3 + c_4 \cdot x_1^2 \\ & + c_5 \cdot x_1 \cdot x_2 + c_6 \cdot x_1 \cdot x_3 \\ & + c_7 \cdot x_2^2 + c_8 \cdot x_2 \cdot x_3 + c_9 \cdot x_3^2. \end{aligned} \tag{9}$$

IV. REAL-TIME IMPLEMENTATION WITH DSP

A. Improvement of SVM Filter: Window Processing

For a real-time system, our goal is to realize an algorithm that can recognize a fall before it is completed. The system must recognize a dangerous action within a very short period of time to ensure that there is enough time for airbag inflation. At the same time, the system should not be falsely triggered when a person is going through normal motions.

We suggest a slide window processing algorithm, i.e., one that defines a certain width of "window" for processing. We cut a selected "window width" for FFT and SVM filter judging, and, at the same time, push the window forward, thus allowing the data in the window to be judged every $1/200$ s.

The experiments carried out showed that the falling motion and the other motions could be totally separated using all these window widths. Fig. 10 shows the classification results in a Matlab figure, in which the blue points represent the fall data and the red points represent the other motions.

B. Improving the SVM Filter: Lowering the Sample Rate

As defined above, the sampling rate of our μIMU is 200 Hz. For the window process algorithm, a new array of six channels of data renews the FFT results of the $60 * 1$ polynomial every 0.005 seconds. Within this very short period of time, the system

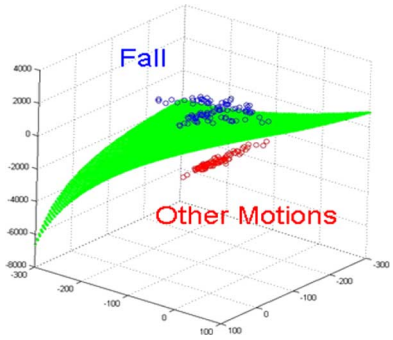

Fig. 10. Falling and other motions can be classified.

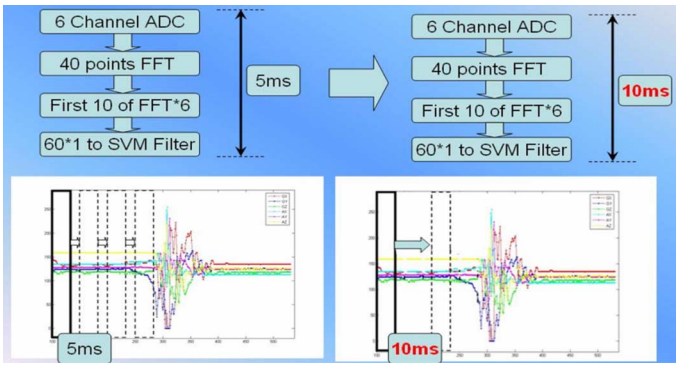

Fig. 11. The filter computations can be performed in 1/100 s.

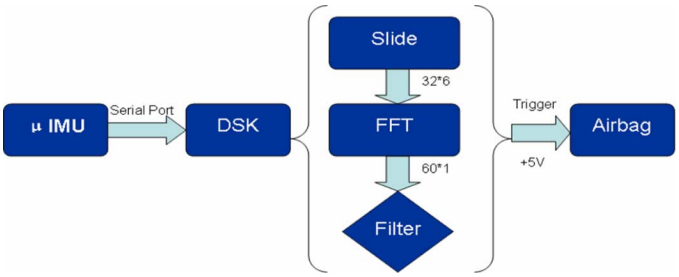

Fig. 12. Real-time recognition structure.

must recognize whether the motion is dangerous, which means the FFT and the SVM filter computations should be completed within 0.005 s.

Fig. 11 shows the computational requirements for this filtering process. In our most updated system, 200 Hz ADC data is transmitted, but the data is sampled and trained every 10 ms. In addition, with the SVM training process, a filter for fall detection is generated. The results show that we can classify falling and other motions clearly. Therefore, this new filter can be loaded to a DSP and the calculation time can be prolonged to 10 ms.

C. DSP Implementation

As described above, for a real product, all the algorithms must be integrated into one chip. For a high-speed DSP, we transfer the data into the DSP first, let the algorithm read the data using the fixed slide window, and then judge each window for danger. Fig. 12 shows the algorithm flow of the system.

The TMS320 6713 DSP chip is used for our system. The C6713 device is based on the high-performance, advanced very-long-instruction-word (VLIW) architecture developed by Texas Instruments (TI), making it an excellent choice for multichannel and multifunction applications. The key issue in selecting a DSP is operating speed, which makes the C6713 device a suitable choice [14].

a) Computation Time Consumption for N-Point FFT: FFT is widely used for frequency domain processing and spectrum analysis. It is a computationally efficient discrete Fourier transform (DFT), which is defined as

$$X(k) = \sum_{N=0}^{N-1} X_n W_N^{kn}, \quad k = 0, \ldots, \mathrm{N}-1 \tag{10}$$

where the twiddle factor is defined as

$$\mathrm{W_N^{kn}} = \mathrm{e}^{-2\mathrm{j}\pi nk/N}. \tag{11}$$

The reduced complexity of the radix-2 FFT algorithms is $(N/2) * \log_2(N)$ complex multiplications and $(N) * \log_2(N)$ complex additions [14]. An experiment shows that FFT simulation based on the radix-2 FFT algorithm (367 111 cycles for a DSP of 300 MHz) will cost around 0.001 s, which is insignificant compared to the time-cost for mechanical systems.

b) SVM Filter Consumption: As mentioned above, we need to generate x_1, x_2 and x_3 before using the SVM filter, as shown in (7). Originally, we had the first ten-order FFTs of the six ADC channels; therefore, a $60 * 1$ polynomial is generated. In the SVM training process, we have one parameter matrix $(60 * 3)$. This $60 * 1$ polynomial is multiplied with the parameter matrix, resulting in a $3 * 1(\mathrm{x_1}, \mathrm{x_2}, \mathrm{x_3})$ polynomial that is ready for the final filter

$$\begin{aligned} f(x_1, x_2, x_3) = {} & c_0 + c_1 \cdot x_1 + c_2 \cdot x_2 \\ & + c_3 \cdot x_3 + c_4 \cdot x_1^2 \\ & + c_5 \cdot x_1 \cdot x_2 + c_6 \cdot x_1 \cdot x_3 \\ & + c_7 \cdot x_2^2 + c_8 \cdot x_2 \cdot x_3 + c_9 \cdot x_3^2. \end{aligned} \tag{9}$$

For the matrix calculation, 180 multiplications and 180 additions are required. For the filtering algorithm, 15 multiplications and 9 additions are needed.

An experiment shows the simulation results of the SVM filter, which includes the $60 * 1$ FFT result, and the number of cycles is about 66 910. A DSP of 300 MHz costs 0.00002 seconds. In the simulation results, the entire consumption of the DSP is 434 021 cycles, whereas in real-time computation, our new filter gives us 3 M cycles for calculation, which is enough if we take the simulation result.

c) Demonstration of DSP Real-Time Recognition: Fig. 13 shows a demo of the DSP system in recognizing a fall motion. An integrated algorithm is embedded in the DSP. The algorithm performs FFT and SVM, which discriminate normal motions (walking, going up stairs, sitting, standing) from falls. As the photos show, the airbag is triggered only when a fall occurs. This

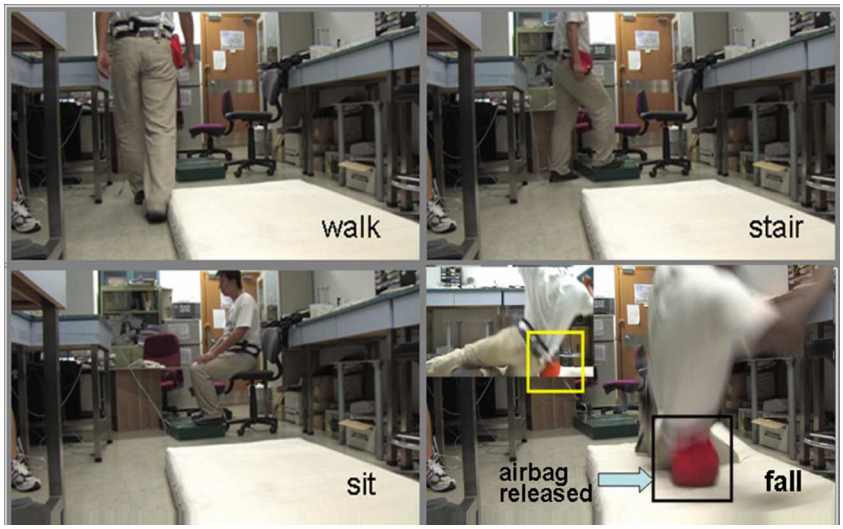

Fig. 13. Demonstration of fall protection in real-time.

demo proves the feasibility of the real-time DSP application and the entire airbag system.

V. Conclusion

This paper presents a novel MEMS-based human airbag system that is under development. A μIMU is used for the detection of complex human motions and the recognition of a falling down motion, which can then be used to trigger the release of airbags. An air release system is also designed. We set up an independent demo to demonstrate that the airbag system is feasible when used in combination with our μIMU. We also use SVM as a pattern recognition method for training after PCA for DFT data. We show that selected eigenvector sets can classify 200 experimental data sets to sort the eigenvectors into "non-falling-down" and "falling down" categories. With the improvement made to our SVM filter, the algorithms can easily be embedded into a real-time DSP. The experiments show that the embedded algorithms can classify falls and non-falls in real time and that the airbag can be deployed when a fall occurs.

References

[1] M. N. Nyan, F. E. H. Tay, T. H. Koh, Y. Y. Sitoh, and K. L. Tan, "Location and sensitivity comparison of MEMS accelerometers in signal identification for ambulatory monitoring," *Electron. Components Technol.*, vol. 1, no. 1–4, pp. 956–960, Jun. 2004.

[2] J. Chan, P. S. Lam, P. C. Sze, and K. S. Leung, "A study of the epidemiology of falls in Hong Kong," in *Proc. Symp. Preventing Falls and Fractures in Older Persons*, Yokohama, Japan, Jul. 2004.

[3] P. Kannus, J. Pakkari, and J. Poutala, "Comparison of force attenuation properties of four different hip protectors under simulated falling conditions in the elderly: An in vitro biomechanical study," *Bone*, vol. 25, pp. 229–235, 1999.

[4] P. C. Sze, "Mechanical and compliance study of a modified hip protector for old age home residents in Hong Kong," M.Phil. thesis, The Chinese Univ. Hong Kong, Hong Kong, China, 2006.

[5] A. K. Nakahara, E. E. Sabelman, and D. L. Jaffe, "Development of a second generation wearable accelerometric motion analysis system," in *Proc.1st JointBMES/EMBS Conf.*, Oct. 1999, vol. 1, no. 13–16, p. 630.

[6] C. V. Bouten, K. T. Koekkoek, M. Verduin, R. Kodde, and J. D. Janssen, "A triaxial accelerometer and portable data processing unit for the assessment of daily physical activity," *IEEE Trans. Biomed. Eng.*, vol. 44, no. 3, pp. 136–147, Mar. 1997.

[7] D. M. Karantonis, M. R. Narayanan, M. Mathie, N. H. Lovell, and B. G. Celler, "Implementation of a real-time human movement classifier using a triaxial accelerometer for ambulatory monitoring," *IEEE Trans. Inf. Technol. Biomed.*, vol. 10, no. 1, pp. 156–167, Jan. 2006.

[8] A. H. F. Lam, W. J. Li, Y. Liu, and N. Xi, "MIDS: Micro input devices system using MEMS sensors," in *Proc. IEEE/RSJ Int. Conf. Intell. Robot Syst.*, Oct. 2002, vol. 2, no. 30, pp. 1184–1189.

[9] A. H. F. Lam, R. H. W. Lam, W. J. Li, M. Y. Y. Leung, and Y. Liu, "Motion sensing for robot hands using MIDS," in *Proc. IEEE Int. Conf. Robot. Autom., ICRA'03*, Sep. 2003, vol. 3, no. 14–19, pp. 3181–3186.

[10] G. Zhang, G. Shi, Y. Luo, H. Wong, W. J. Li, P. H. W. Leong, and M. Y. Wong, "Towards an ubiquitous wireless digital writing instrument using MEMS motion sensing technology," in *Proc. IEEE/ASME Int. Conf. Adv. Intell. Mechatron.*, 2005, pp. 795–800.

[11] M. Barlett and T. Sejnowski, "Independent componets of face images: A representation for face recognition," in *Proc. 4th Annu. Joint Symp. Neural Comput.*, Pasadena, CA, May 17, 1997.

[12] N. Cristianini and J. Shawe-Taylor, *An Introduction to Support Vector Machines and Other Kernel-Based Learning Methods*. Cambridge, U.K.: Cambridge Univ. Press, 2000.

[13] Analog Devices Inc., Precision $\pm$1.7 g Single/Dual Axis Accelerometer ADXL203 Datasheet 2004.

[14] [Online]. Available: www.ti.com

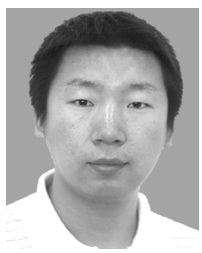

Guangyi Shi received the B.Eng. and M.Eng. degrees in mechatronics engineering from the Beijing Institute of Technology, Beijing, China, in 2001 and 2004, respectively, and the Ph.D. degree in mechanical and automation engineering from the Chinese University of Hong Kong, Hong Kong, China, in 2007.

His research interests include MEMS sensor applications, multiple human motions tracking and identification.

Dr. Shi received the Best Student Paper Award of 2007 IEEE International Conference on Robotics and Biomimetics (ROBIO).

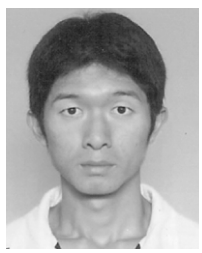

Cheung Shing Chan received the B.Eng. degree in mechanical engineering from the Chinese University of Hong Kong (CUHK), Hong Kong, China, in 2005, and the M.Med. degree from the Department of Orthopaedics and Traumatology, CUHK, in 2007.

His research interests include fall-kinematics and mechanical design of compact protecting system against falling for the elderly.

Wen J. Li received the B.S. and M.S. degrees from the University of Southern California, Los Angeles, in 1987 and 1989, respectively, and the Ph.D. degree from the University of California, Los Angeles, in 1997, all in aerospace engineering.

He is currently a Full Professor and Head of the Centre for Micro and Nano Systems, CUHK. His research interests are in the fields of advanced MEMS applications and nanoscale sensing, manipulation, and assembly.

Dr. Li's research group has received several awards from major IEEE conferences, including IEEE-ICRA 2003 (Best Conference Paper), IEEE-NANO 2003 (Best Student Poster Paper), and IEEE/ASME AIM 2007 (Best Conference Paper). He has served as a guest editor for several IEEE technical publications and is currently the Editor-in-Chief of the *IEEE Nanotechnology Magazine*. He has also served as the General Chair of IEEE-NANO 2007, Organizing Chair of IEEE-NEMS 2006 and General Chair of IEEE-ROBIO 2005.

Kwok-Sui Leung received the M.D. degree from the Chinese University of Hong Kong, Hong Kong, China, in 1991.

He is a Professor at the Department of Orthopaedics and Traumatology, Chinese University of Hong Kong, for more than 20 years. He is also a Consultant in Traumatology in the Prince of Wales Hospital, Shatin, Hong Kong. His research work includes fracture healing, biochemistry and enhancement methods, biological response to mechanical stimulation, fragility fracture fixation and prevention, and computer-aided orthopaedic surgery.

Yuexian Zou received the M.Sc. degree in 1991 and the Ph.D. degree in 2000 from the University of Electronic Science and Technology of China, Chengdu, and the University of Hong Kong, Hong Kong, China, respectively.

She serves as an Associate Professor in Peking University. She is currently working on array signal processing and video signal processing projects. Her research interests include digital filter design, adaptive signal processing, pattern recognitions, and MEMS sensor applications.

Yufeng Jin received the Ph.D. degree from Southeast University, Nanjing, China, in May 1999.

He is Director of the National Key Laboratory of Micro/Nano Fabrication Technology, China. He is now a Professor at the Institute of Microelectronics, Peking University, China. His research interests focus on numerical simulation for microfluid within a ministructure, RF MEMS including microwave MEMS switch, high Q tunable capacitor, resonator and circuit. Research interests also include advanced MEMS packaging technology. Current packaging research is mainly focused on MEMS vacuum packaging, microsensor, 3-D integration of microelectronics and its application systems.